



# Collective behavior of composite active particles

Joshua Eglinton , Mike I. Smith , and Michael R. Swift

*School of Physics and Astronomy, University of Nottingham, Nottingham NG7 2RD, United Kingdom*



(Received 20 August 2021; accepted 29 March 2022; published 26 April 2022)

We describe simulations of active Brownian particles carried out to explore how dynamics and clustering are influenced by particle shape. Our particles are composed of four disks, held together by springs, whose relative size can be varied. These composite objects can be tuned smoothly from having a predominantly concave to a convex surface. We show that even two of these composite particles can exhibit collective motion which modifies the effective Peclet number. We then investigate how particle geometry can be used to explain the phase behavior of many such particles.

DOI: [10.1103/PhysRevE.105.044609](https://doi.org/10.1103/PhysRevE.105.044609)

## I. INTRODUCTION

There is currently significant interest in the dynamics of active matter and the modeling of collective biological motion [1]. Active particles take their energy from their surroundings to induce directed motion. Natural examples of collective motion in active systems include the flocking of birds, shoals of fish, and clustering in bacterial colonies [2]. Within the physics community, active matter represents a statistical system driven far from equilibrium which can exhibit nonequilibrium ordering and phase transitions [3]. However, to date, there is no overarching framework to describe such phenomena.

Much of the theoretical work in this field has focused on collections of freely rotating disks or spheres [4,5]. Under appropriate conditions, such systems can exhibit clustering, often referred to as motility-induced phase separation (MIPS) [6]. This transition results from a competition between the rate of arrival of particles in a region of space and the ability of particles to rotate and leave [7,8]. In these systems the addition of aligning interactions is known to enhance clustering [9], while attractive interactions can significantly influence the collective behavior [10,11].

These ideas have been explored in more complex systems via experiments and simulations to investigate asymmetric active particles including rods [12–14], dumbbells [15], and composite or continuum systems [16–18]. It is now realized that particle shape can have a significant influence on the collective dynamics.

One further feature that active systems have in common is the strong coupling between the particles' dynamics and their interaction with boundaries [19]. It is known that active systems can drive nonequilibrium interfacial fluctuations [20], exhibit nonideal pressure variations [21], and show clustering effects induced by the presence of a boundary [22]. Intriguingly, the convex or concave nature of the boundary can have a pronounced effect on the clustering that is observed [23].

In this article we describe simulations of an active particle system in which the shape of the particles can be changed continuously. Specifically, we consider particle shapes which have surfaces that possess both concave and convex regions.

We investigate how this structure influences the dynamics of a small number of particles and the collective behavior of many such particles.

## II. MODEL

Our basic active particle is constructed out of four disks, as illustrated in the insets to Fig. 1. The disks are held together by five springs so that the composite particle, referred to as a “diamond,” moves as a solid body. The head (blue) and tail (red) particles have a radius  $R = 1$  which defines the natural length scale. The two side disks (green) have radius  $a$  that is varied to alter the shape of the diamonds. The diamonds are assumed to be governed by overdamped dynamics. While this approach does not consider a full hydrodynamic treatment of the problem, it approximates the motion of a nonspherical particle in a viscous liquid. The equation of motion of disk  $i$  within a diamond is

$$\frac{d\mathbf{r}_i}{dt} = V_0 \hat{\mathbf{n}}_i + \mu \sum_j \mathbf{F}_{ij}, \quad (1)$$

where  $\mathbf{r}_i$  is the coordinate of the disk,  $V_0$  is the speed due to the active force,  $\hat{\mathbf{n}}_i$  is a unit vector from the tail to the head,  $\mu$  is the mobility parameter, and  $\mathbf{F}_{ij}$  is the radial harmonic interaction force  $-k(|\mathbf{r}_i - \mathbf{r}_j| - R_i - R_j)\hat{\mathbf{r}}_{ij}$  between pairs of disks. This force maintains a fixed separation between disks within a diamond. Here,  $R_i$  and  $R_j$  are the radii of the disks,  $k$  is the spring constant, and  $\hat{\mathbf{r}}_{ij}$  is a unit vector from disk  $j$  to disk  $i$ . In our simulations we have defined  $V_0 = 1$ , and used values of  $\mu = 1$ ,  $k = 100$ , and a time step  $\Delta t = 10^{-3}$  time units. Reducing the time step did not strongly influence the observed behavior.

The active force that acts on each disk results in a speed  $V_0$  for the diamond as a whole. In order to ensure solid body motion, we have assumed that the mobility parameter  $\mu$  that relates force to velocity is the same for all disks, irrespective of their size or position within the diamond. If a constant torque  $\tau_r$  is applied to the diamond, then the resulting constant angular velocity  $\omega$  is readily shown to be given by  $\omega = \mu \tau_r / 2(R + a)^2$ . Even though inertia is ignored in this

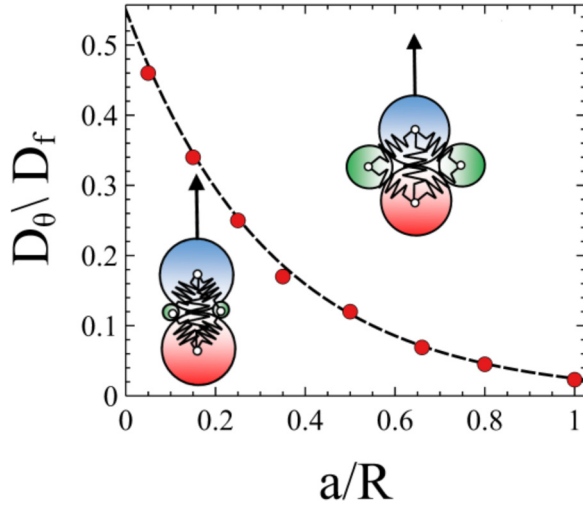


FIG. 1. The insets show the configuration of two composite particle “diamonds” with different values of the shape parameter  $a/R$ , as indicated by their positions on the  $x$  axis. The springs ensure that the diamonds move as solid objects. An active force is added to each disk in the direction from the tail (red) to the head (blue). A random force is added to the head and tail disks to induce angular diffusion. The main panel shows the variation of the ratio of the angular and linear diffusion coefficients as a function of  $a/R$ .

overdamped limit, there is resistance to rotation that is shape dependent. This behavior arises because larger side particles are located further from the center of the diamond. For a given rotational speed they must therefore move faster, thus increasing the required torque.

In order to introduce rotational diffusion, an additional random force is added in Eq. (1) to the head and tail disks; each force component  $\eta_\alpha$  is assumed to be Gaussian with correlator  $\langle \eta_\alpha(t) \eta_\beta(t') \rangle = 2D_f \delta_{\alpha,\beta} \delta(t - t')$ , where  $\alpha$  and  $\beta$  are Cartesian coordinates and  $D_f$  is a linear diffusion constant that characterizes the fluctuation of the applied force. The resulting angular fluctuations can be measured and are found to be diffusive with angular diffusion constant  $D_\theta$ . From simulations of single diamonds, we find that  $D_\theta$  and  $D_f$  are related to the ratio  $a/R$  as shown in the main panel of Fig. 1. In what follows we define a linear Peclet number resulting from the applied random force  $Pe^f = V_0 R / D_f$ . The corresponding angular Peclet number  $Pe^\theta = V_0 / R D_\theta$  can be obtained from the data shown in Fig. 1. In our simulations we keep  $V_0 = 1$  fixed and vary the noise strength to change the Peclet number.

A single diamond behaves as an active Brownian particle with speed  $V_0$  and angular diffusion  $D_\theta$ . If two diamonds collide, they are assumed to repel due to repulsive springs which act radially between overlapping disks. The response to these forces is also treated in the overdamped limit, with the size-independent mobility parameter  $\mu$  and the spring constant  $k$  as above.

### III. FEW-BODY DYNAMICS

A distinctive feature of this study is that the diamonds, as a result of their shape, can lock together, exhibiting collective dynamics of as few as two particles. For example, consider

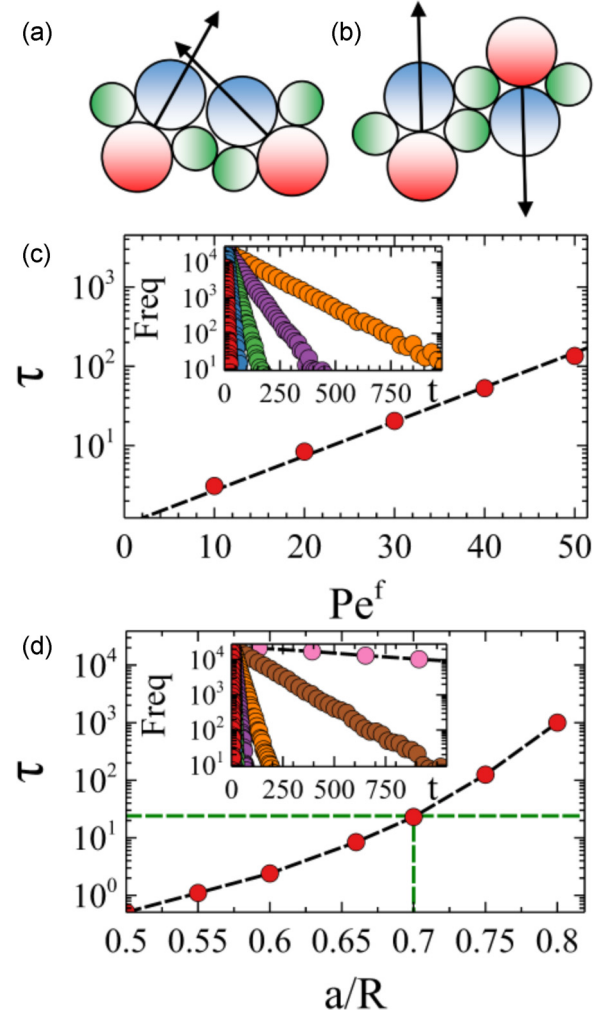


FIG. 2. The upper panel shows two possible configurations for a pair of diamonds: (a) glider configuration, and (b) spinner configuration. The glider is stable and propagates in the direction of the two head particles. The spinner does not propagate but rotates on the spot. The survival time distributions for stable rotation are shown in the insets to (c) and (d), for a range of Peclet numbers and  $a/R$ . The observed exponential decay can be characterized by a lifetime  $\tau$  shown in the main panels of (c) and (d). The stability of the spinners grows exponentially with increasing Peclet number and grows even more strongly with increasing  $a/R$ . The horizontal line in (d) shows when the lifetime of a spinner becomes comparable with the time taken for a diamond to travel from one cluster to the next, as discussed in the main text.

the configurations shown in Fig. 2. The individual diamonds are constructed from disks with a size ratio  $a/R = 2/3$ . This is the closest shape that mimics a single disk; namely, a circle of radius  $2R$  just enclosing the diamond. In the left-hand configuration [Fig. 2(a)], the two diamonds lock together in such a way that the pair move together at a constant speed but the angular fluctuations are somewhat suppressed. Such an object travels around a periodic system indefinitely, resembling a “glider” configuration in Conway’s Game of Life [24]. The effective  $Pe^\theta$  is much increased because of the suppression of angular fluctuations due to the rotational resistance.

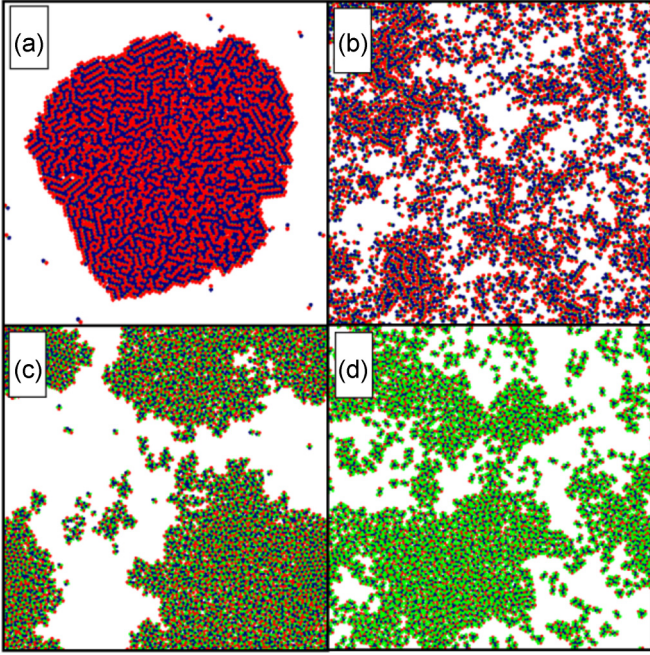


FIG. 3. Snapshots taken from simulations in the steady state for different values of the shape parameter  $a/R$ : (a)  $1/20$ , (b)  $1/4$ , (c)  $2/3$ , and (d)  $4/5$ .

On the other hand, the right-hand configuration [Fig. 2(b)] allows the pair of particles to remain in contact and rotate on the spot, suppressing translational motion. Such a configuration is long lived due to the lack of inertia in the overdamped limit. These “spinners” eventually separate with a survival time that is given by an exponential distribution. The lifetime is found to depend on the  $Pe^f$ , as shown in Fig. 2(c). The exponential growth of the lifetime with  $Pe^f$  exhibits an Arrhenius behavior with the noise playing the role of an effective temperature. High  $Pe^f$  spinners thus remain stable in these configurations for longer, resulting in a reduced effective Peclet number compared with an isolated diamond. Figure 2(d) also shows how the lifetime of a spinner depends on the shape parameter  $a/R$ . The dependence is even greater than exponential. Given this strong influence of particle shape on few-body systems, we now ask how shape effects influence the collective behavior of many-particle systems.

#### IV. COLLECTIVE BEHAVIOR

The shape of the diamond is controlled by the ratio  $a/R$ . For  $a/R < 1/4$  the side surface is concave; in the limit  $a/R \rightarrow 0$  the diamond resembles a dumbbell. For  $a/R = 1/4$  the diamond has sides that are relatively flat, mimicking a short rod. As noted above, for  $a/R = 2/3$ , the diamond corresponds as closely as possible to a circle, whereas for  $a/R > 2/3$  the side lobes start to dominate. We have simulated multiple diamonds for a range of  $a/R$ . Each system has 2500 diamonds and the region has a size  $L$  so that a 50% by area filling fraction is maintained. This definition ignores small variations due to excluded area effects. Periodic boundary conditions are employed in both directions.

Figure 3 shows a series of snapshots taken in the steady state for four different values of  $a/R$ , all at  $Pe^f = 20$ . Figure 3(a) is for  $a/R = 1/20$ . Here, a dense crystalline cluster forms which slowly rotates about its center. Figure 3(b) is for  $a/R = 1/4$ . In this case there are only short-lived transient clusters and the system remains homogeneous on the average over time. In Fig. 3(c),  $a/R = 2/3$ , and a dynamic, fluidlike cluster persists with accompanying swirling motion. Finally, Fig. 3(d) is for  $a/R = 4/5$  in which the tendency to form large clusters appears less pronounced than for  $a/R = 2/3$ . It is also striking that in between the clusters there are significant numbers of spinners such as the ones investigated in Fig. 2. For movies, see the Supplemental Material [25].

In active systems with no attractive interactions, clustering results from steric hindrance and a competition between the rate at which particles arrive in and leave from a region of space (MIPS). For simple disks, MIPS is controlled by the filling fraction and the Peclet number.

In order to quantify the observed behavior in the diamond model, we have defined an order parameter to measure density fluctuations. Specifically, we calculate a coarse-grained density map based on the center of each diamond. We divide the system into 400 square regions  $i$  and count the number of diamonds in each region at a particular time  $t$ ,  $N_{i,t}$ . The system is allowed to relax for 9000 time units and we then calculate the time-averaged variance of these number fluctuations over the next 1000 time units,  $\langle N_{i,t}^2 \rangle - \langle N_{i,t} \rangle^2$ , where the angular brackets denote the average over spatial regions and time. Such a measure is sensitive to the overall structure but is not influenced by the collective motion of the clusters.

In the case of our noncircular particles, the ability of a diamond to push past a neighboring diamond or to leave a cluster depends on the particle geometry. In addition, the tendency of a particle to propagate can be hindered by local ordering as, for example, in the case of the spinners. Consequently, the phase diagram has a rich structure.

Figure 4 shows the phase diagram in the space of  $(a/R, Pe^f)$  for a fixed filling fraction of 50%. At small  $a/R$  the particles enter a crystallized arrangement which persists up to a  $a/R$  of 0.2. A crystal represents the highest density packing of particles composed of two spheres. This high density suppresses fluctuations resulting in a very stable configuration that enhances MIPS by preventing the rearrangement of particles. Figure 3(a) illustrates this, where particles once joined to the main cluster remain attached. Such behavior is similar to that observed in active dumbbells [15]. The addition of small side particles does not disrupt the possibility of this configuration provided  $a/R \leq 0.2$ . This is because the side particles are not big enough to prevent a close packed arrangement of the larger particles. There is therefore no strain applied to the crystal configuration. As the side particles increase slightly above  $a/R = 0.2$  (the sides are still concave at this point) the large particles are forced slightly further apart. This creates a strain in the crystal, which decreases the stability of the packing. Fluctuations due to particle noise allow the relative position of particles to move more easily.

The limiting case for this crystallization occurs when  $a/R \sim 0.25$ . At this point the edge of the small particle is aligned with the tangent to the two larger particles. As two particles come together they cannot interlock, simply sliding



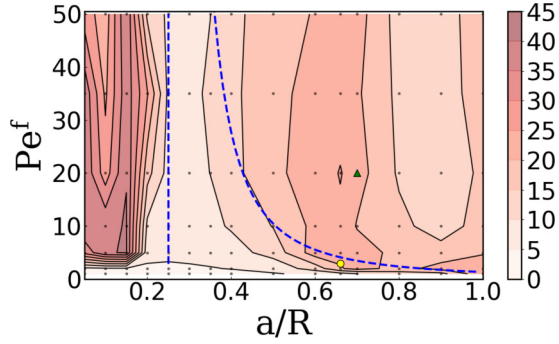


FIG. 4. Phase diagram showing the degree of clustering as a function of Peclet number  $Pe^f$  and shape parameter  $a/R$ . The color scheme goes from low (light) to high (dark) degrees of clustering, as measured by the order parameter defined in the main text. The yellow circle represents the expected onset of MIPS for circular disks. The green triangle shows where the spinner lifetime is approximately equal to the time taken to travel between clusters at  $Pe^f = 20$ . The dotted blue lines represent expected transitions in behavior based on geometrical arguments (see details in the main text). The black dots represent individual simulation runs.

past one another. The phase diagram in Fig. 4 indicates that this coincides with a dramatic decrease in stable clustering. The left-hand side of this diagram can therefore be understood in purely geometrical terms.

As  $a/R \rightarrow 2/3$ , the diamonds, as closely as possible within this model, resemble disks and a transition analogous to MIPS for disks results. The onset of clustering occurs at a value of the  $Pe^\theta$  in close agreement with that obtained in disk simulations [4]. The yellow dot in Fig. 4 shows this point in terms of the corresponding  $Pe^f$  obtained from Fig. 1. Around this value of  $a/R$  there is an extended region in the phase diagram of MIPS-like clustering. However, if circular particles are made even slightly ellipsoidal, it is known that the MIPS mechanism breaks down [18]. This occurs because any noncircular shape experiences a torque about its center of mass that disrupts the polar boundary layer. In contrast, our diamonds *can* maintain a polar boundary layer. We now demonstrate that this difference arises due to the surface of a diamond having both concave and convex regions, allowing the interlocking of particles.

The boundary between rodlike (transient clusters) and disklike (MIPS) behavior can be estimated by considering the time taken for one diamond to move past another. From simple trigonometry, the distance a side lobe protrudes beyond the tangent to the two large disks (Fig. 1) is  $\Delta = R|(2\alpha + \alpha^2)^{1/2} + \alpha - 1|$ , where  $\alpha = a/R$ . Over a time  $t$  the sideways motion is diffusive, so to travel a distance  $\Delta$  requires a time given by the equation  $\Delta^2 = 2D_f t$ . This time can be compared with the one required for two diamonds to travel passed one another ( $t = 2R/V_0$ ). This comparison gives an estimate of the boundary between sliding and locking motion. In terms of  $Pe^f$

we find  $Pe^f = 4/[(2\alpha + \alpha^2)^{1/2} + \alpha - 1]^2$ . This simple model, with no adjustable parameters, is shown by the right-hand dotted blue line on Fig. 4, in good agreement with the simulated data.

Increasing  $a/R$  further results in a weakening of the tendency to cluster, this despite the apparent increase in stability of the two diamond configurations with increasing  $a/R$ . In Fig. 3(d) and the corresponding movies in the Supplemental Material one does not observe a significant number of the glider configuration [cf. Fig. 2(a)]. Though the more stable of the two diamond configurations, any gliders that form quickly disintegrate as they collide with larger clusters. However, a large number of the spinning configurations, together with other small clusters of three or four, are observed. Once a pair of diamonds forms a spinner they no longer propagate, as shown in Fig. 2(d), thus reducing the effective Peclet number of the entire system. This reduction in number of free particles contributes to a decreased stability of the larger clusters.

To test this idea we estimate where the spinner survival time might start to become significant when compared to the time taken for a diamond to propagate between clusters. To determine a typical distance between clusters, we assume that all particles occupy a circular region with a filling fraction of 0.8 (for loosely packed disks). If the total area filling fraction is  $\phi = 1/2$ , then the area of the cluster is  $A_c = \phi L^2/0.8$ , giving a radius  $R_c = (\phi L^2/0.8\pi)^{1/2}$ . The corresponding distance between clusters is  $L - 2R_c \approx 24$ . From Fig. 2(d) this gives an  $a/R$  value of about 0.7 as shown by the green triangle in Fig. 4, confirming the significance of localized spinning clusters for the decrease in degree of clustering for higher values of  $a/R$ .

## V. CONCLUSIONS

Our simulations highlight the importance of shape in active matter systems. The topology of our diamonds give rise to a range of novel collective behaviors. It is shown that even two particles can result in spinning clusters with lifetimes that exhibit an Arrhenius-like dependence on the Peclet number and a strong dependence on the shape parameter  $a/R$ . MIPS-induced clustering is observed for a wide range of  $a/R$  and can be predicted using simple scaling arguments. The fact that MIPS is suppressed for high  $a/R$  also shows the role of few-body interactions; small clusters can form but they do not propagate, reducing the effective Peclet number. Convex and concave particle shapes may be particularly relevant in soft active matter, where interparticle forces can result in complex deformations. Phase behavior in such systems is likely to differ significantly from that of the simple particle geometries more commonly studied.

## ACKNOWLEDGMENT

M.I.S. gratefully acknowledges support from the Royal Society via a University Research Fellowship.

- [1] G. Popkin, The physics of life, *Nature (London)* **529**, 16 (2016).
- [2] M. C. Marchetti, J. F. Joanny, S. Ramaswamy, T. B. Liverpool,

- J. Prost, M. Rao, and R. A. Simha, Hydrodynamics of soft active matter, *Rev. Mod. Phys.* **85**, 1143 (2013).

- [3] H. Jaeger and A. J. Liu, Far-from-equilibrium physics: An overview, [arXiv:1009.4874](#).
- [4] Y. Fily, S. Henkes, and M. C. Marchetti, Freezing and phase separation of self-propelled disks, [Soft Matter](#) **10**, 2132 (2014).
- [5] G. S. Redner, M. F. Hagan, and A. Baskaran, Structure and Dynamics of a Phase-Separating Active Colloidal Fluid, [Phys. Rev. Lett.](#) **110**, 055701 (2013).
- [6] M. E. Cates and J. Tailleur, Motility induced phase separation, [Annu. Rev. Condens. Matter Phys.](#) **6**, 219 (2015).
- [7] A. P. Solon, J. Stenhammar, M. E. Cates, Y. Kafri, and J. Tailleur, Generalized thermodynamics of motility-induced phase separation: Phase equilibria, Laplace pressure, and change of ensembles, [New J. Phys.](#) **20**, 075001 (2018).
- [8] S. C. Takatori and J. F. Brady, Towards a thermodynamics of active matter, [Phys. Rev. E](#) **91**, 032117 (2015).
- [9] E. Sesé-Sansa, I. Pagonabarraga, and D. Levis, Velocity alignment promotes motility-induced phase separation, [Europhys. Lett.](#) **124**, 30004 (2018).
- [10] J. Schwarz-Linek, C. Valeriani, A. Cacciuto, M. E. Cates, D. Marenduzzo, A. N. Morozov and W. C. K. Poon, Phase separation and rotor self-assembly in active particle suspensions, [Proc. Natl. Acad. Sci. USA](#) **109**, 4052 (2012).
- [11] G. S. Redner, A. Baskaran, and M. F. Hagan, Reentrant phase behavior in active colloids with attraction, [Phys. Rev. E](#) **88**, 012305 (2013).
- [12] For a review, see M. Bär, R. Grossmann, S. Heldenreich, and F. Peruani, Self-propelled rods: Insights and perspectives for active matter, [Annu. Rev. Condens. Matter Phys.](#) **11**, 441 (2020).
- [13] K. H. Nagai, Collective motion of rod-shaped self-propelled particles through collision, [Biophys. Physicobiol.](#) **15**, 51 (2018).
- [14] V. Narayan, S. Ramaswamy, and N. Menon, Long-lived giant number fluctuations in a swarming granular nematic, [Science](#) **317**, 105 (2007).
- [15] L. F. Cugliandolo, P. Digregorio, G. Gonnella, and A. Suma, Phase Coexistence in Two-Dimensional Passive and Active Dumbbell Systems, [Phys. Rev. Lett.](#) **119**, 268002 (2017).
- [16] S. Weitz, A. Deutsch, and F. Peruani, Self-propelled rods exhibit a phase-separated state characterized by the presence of active stresses and the ejection of polar clusters, [Phys. Rev. E](#) **92**, 012322 (2015).
- [17] A. M. Menzel and T. Ohta, Soft deformable self-propelled particles, [Europhys. Lett.](#) **99**, 58001 (2012).
- [18] R. Großmann, I. S. Aranson, and F. Peruani, A particle-field approach bridges phase separation and collective motion in active matter, [Nat. Commun.](#) **11**, 5365 (2020).
- [19] C. Bechinger, R. Di Leonardo, H. Lowen, C. Reichhardt, G. Volpe, and G. Volpe, Active particles in complex and crowded environments, [Rev. Mod. Phys.](#) **88**, 045006 (2016).
- [20] G. Junot, G. Briand, R. Ledesma-Alonso, and O. Dauchot, Active versus Passive Hard Disks against a Membrane: Mechanical Pressure and Instability, [Phys. Rev. Lett.](#) **119**, 028002 (2017).
- [21] A. P. Solon, J. Stenhammar, R. Wittkowski, M. Kardar, Y. Kafri, M. E. Cates, and J. Tailleur, Pressure and Phase Equilibria in Interacting Active Brownian Spheres, [Phys. Rev. Lett.](#) **114**, 198301 (2015).
- [22] A. Deblais, T. Barois, T. Guerin, P. H. Delville, R. Vaudaine, J. S. Lintuvuori, J. F. Boudet, J. C. Baret, and H. Kellay, Boundaries Control Collective Dynamics of Inertial Self-Propelled Robots, [Phys. Rev. Lett.](#) **120**, 188002 (2018).
- [23] N. Kumar, Trapping and sorting of active particles: Motility-induced condensation and smectic defects, [Phys. Rev. E](#) **99**, 032605 (2019).
- [24] M. Gardiner, The fantastic combinations of John Conway's new solitaire game "life", [Sci. Am.](#) **223**, 120 (1970).
- [25] See Supplemental Material at <http://link.aps.org/supplemental/10.1103/PhysRevE.105.044609> for movies showing the dynamics.